https://doi.org/10.2352/ISSN.2470-1173.2019.3.SDA-631

Thin Form-Factor Super Multiview Head-Up Display System

Ugur Akpinar, Erdem Sahin, Olli Suominen, Atanas Gotchev; Tampere University, Tampere, Finland

Abstract

We propose a virtual-image head-up display (HUD) based on the super multiview (SMV) display technology. Implementation-wise, the HUD provides a compact solution, consisting of a thin form-factor SMV display and a combiner placed on the windshield of the vehicle. Since the utilized display is at most few centimeters thick, it does not need extra installation space that is usually required by most of the existing virtual image HUDs. We analyze the capabilities of the proposed system in terms of several HUD related quality factors such as resolution, eyebox width, and target image depth. Subsequently, we verify the analysis results through experiments carried out using our SMV-HUD demonstrator. We show that the proposed system is capable of visualizing images at the typical virtual image HUD depths of $2-3m$*, in a reasonably large eyebox, which is slightly over* $30cm$ *in our demonstrator. For an image at the target virtual image depth of* $2.5m$*, the field of view of the developed system is* $11°x16°$ *and the spatial resolution is around* $240x60$ *pixels in vertical and horizontal directions, respectively. There is, however, plenty of room for improvement regarding the resolution, as we actually utilize an LCD at moderate resolution* $(216ppi)$ *and off-the-shelf lenticular sheet in our demonstrator.*

Introduction

A head-up display (HUD) is a semi-transparent display that shows the visual data to the viewer without requiring to shift gaze from the actual viewpoint. Although HUDs were first originated to be used in military applications [8], they have been also utilized widely for non-military applications, such as automobiles etc. In automotive applications, HUDs can be used either to show some guiding information such as speed or navigation signs [17], or to enhance the vision, e.g. for driving at night or in winter [13]. Their benefit of maintaining the gazing of the driver on the road has been proven to provide safer driving conditions [12, 11]. In automobiles, typical direct projection HUDs [7] reflect the image on the windshield or a separate reflective surface. On the other hand, virtual image HUDs, which rely on various techniques such as relay optics [1], stereo-view type display [14] or holography [3, 5], display the desired information behind the windshield to further reduce the reaccommodation time between the outside world and the shown information. Each of such techniques has different pros and cons. The stereo-view display technique delivers only the binocular cues by providing stereo images to the driver's eyes, which considerably limits the head motion (unless head tracking is utilized) due to predefined zones for the left and right eyes. Moreover, other depth cues, i.e. motion parallax and accommodation are not delivered, which are effective for typical automobile HUD image range of $2-3m$. The relay optics or holographic techniques, on the other hand, correctly deliver all depth cues. However, they usually require large volume of space for optical relay components and/or eyebox expanders. Thus, a compact and easy-to-implement HUD solution, which stimulates all depth cues correctly at the target virtual image distance is desirable.

Vergence, binocular disparity, motion parallax and accommodation constitute the physiological depth cues that the human visual system relies on [15]. All these cues are effective at the typical depth range for virtual HUD images, i.e. $2-3m$, and thus they should be delivered correctly. In this paper, we propose to utilize the super multiview (SMV) display technique as a compact virtual HUD solution, which consists of a few centimeters thick SMV display and a combiner, yet capable of providing all these physiological depth cues. Previously, Takaki et. al. [16] have utilized the SMV technique in the HUD application for long distance image presentation. In order to achieve the desired long depth ranges (e.g. up to 50m), they employ a Fresnel lens placed over the SMV display, which results in a large form-factor design (with thickness of few tens of centimeters) for practical purposes. In this paper, we rather aim to present information at a relatively shorter depth range of $2-3m$, which is the depth range of virtual HUDs. For this depth range, we theoretically analyze the capability of SMV technique in terms of resolution, depth perception, eyebox, etc. Then, we present our SMV-HUD demonstrator that verifies the theoretical analysis.

SMV-HUD

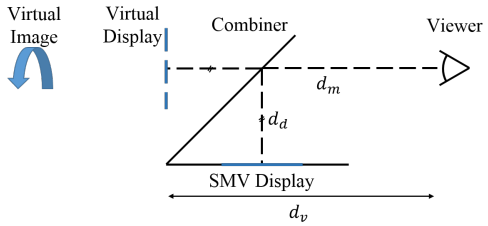

Figure 1: The overall design of the proposed SMV-HUD system.

A HUD system typically consists of two components: the image generation unit produces the image to be displayed to the viewer (driver) and the optical combiner merges this image with the outside world. The display technique used in the image generation unit determines the characteristics of the HUD. The proposed SMV-HUD system consists of a SMV display as the image generation unit and it aims at implementing virtual-image HUD as illustrated in Fig. 1. The distance of the driver from the windshield, d_m, is the common parameter for different HUD types, whereas the distance between the windshield and the image generation unit, d_d, may vary. When the combiner is removed and the display is assumed to be at the virtual display plane (at distance $d_v = d_m + d_d$ from the viewer), the SMV-HUD system in Fig. 1 can be parametrized as shown in Fig. 2.

As illustrated in Fig. 2, a SMV display system can be modeled by two parallel planes representing the lens array plane t and (2D) display plane y, where the system is characterized by (effec-

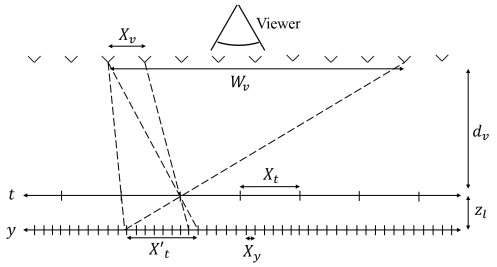

Figure 2: HUD system based on the SMV technique, combiner in Fig. 1 is removed for simplicity.

tive) pixel pitch X_y, lens pitch X_t, and lens thickness z_l. These system parameters determine the perceived resolution and depth of the 3D images, and the available field of view (FOV) at viewing distance d_v within the region where the viewer can move freely, i.e. eyebox W_v. Those user experience aspects, in a sense, constitute the quality factors of a HUD. Furthermore, the interview distance X_v is a critical SMV display parameter especially for (correct) depth perception, as will be discussed in the following section.

Due to the periodicity of the lens array, the viewing zones of the SMV display are also periodic, and one period is considered as the eyebox, which is calculated as

$$W_v = \frac{X_t' d_v}{z_l} = X_t \frac{(d_v + z_l)}{z_l}, \tag{1}$$

where $X_t' = X_t(d_v + z_l)/d_v$ is defined as the multiplexing period. Thus, assuming that the viewing distance d_v is determined according to drivers positioning, which can be fixed to e.g. $90cm$, the eyebox is mainly dependent on the lens pitch. That is, the eyebox can be made larger by increasing the lens pitch. The horizontal FOV, on the other hand, is simply given as

$$\theta_y = 2\arctan\left(\frac{W_y}{2d_v}\right), \tag{2}$$

where W_y is the width of the display. The vertical FOV can be found similarly.

The perceived virtual image resolution and depth are the two key aspects of the SMV-HUD that deserve detailed discussion. In the following sections, those factors are analyzed in detail.

Depth Perception in SMV-HUD

Although the appropriate image distance in virtual HUDs has been a debatable topic, typically, the image depth for automobile HUDs is in the range of $2-3m$. Indeed, the image depth range $2.5-4m$ of a virtual HUD is reported to be ideal for a comfortable viewing experience, i.e. it is expected to meet the needs of all drivers e.g. at different ages [6]. Thus, considering a viewing distance of around $d_v = 90cm$ (to the virtual display plane), the SMV display should deliver all necessary depth cues correctly for an image at $1-2m$ behind the display. In particular, all physiological depth cues, namely vergence, binocular disparity, motion parallax and accommodation, are effective at this target virtual image distance [15]. Delivering the correct binocular cues is simply achieved by providing correct parallax images to the two eyes of the viewer within the eyebox, as one could also achieve e.g. via conventional 3D displays such as multiview and stereoscopic displays. However, unlike such displays, SMV displays are capable of providing smooth motion parallax and also evoking the accommodation cue. These aspects are particularly critical (especially the former one) for the HUD application so as to provide a comfortable undistracted viewing experience to the driver, e.g. without image jumps when the head is moved within the eyebox. The accommodation and motion parallax cues are, thus, discussed below in more detail.

SMV displays are capable of evoking the accommodation response and thus delivering accommodation cue [9]. This is achieved by providing at least two light rays from a virtual image point to each eye of the viewer, which is called as the super multiview condition [10]. Thus, considering the parameters in Fig. 2, the following relation should be satisfied in order to evoke the accommodation cue:

$$X_v = \frac{X_y d_v}{z_l} < W_e, \tag{3}$$

where W_e is the human eye pupil size, which is in $2-8mm$ and typically around 5mm. Providing (sufficiently) accurate accommodation cue is critical first, to avoid (or reduce) the accommodation-vergence conflict that will, otherwise, cause visual discomfort; and second, to reduce the reaccomodation demand between the displayed image and outside world. The first one constitutes problem especially in prolonged use, e.g. as in 3D-TV applications, where there is a non-neglible mismatch between the accommodation and vergence responses. The latter one is a more emphasized problem in the context of HUDs. Both issues can be addressed by evoking the accommodation response in the range of $2.5-4m$ and sufficiently close to the intended image depth, which is perceived via the binocular cues. In this paper we consider the super multiview condition as a measure for accurate accommodation response. However, we believe that both the theoretical analysis and experimental verification of accommodation response deserve more thorough discussion in the context of SMV displays, as there are several other factors affecting the accommodation response such as the distance between the 3D image and the display surface. We consider further theoretical discussion and experimental accommodation measurements out of scope of this paper.

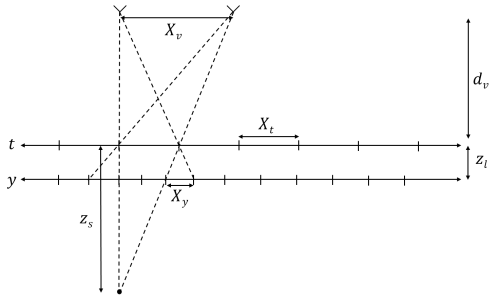

Figure 3: Maximum distance providing smooth motion parallax.

The first condition for the SMV-HUD to provide smooth (continuous) motion parallax is that $X_v \leq W_e$ so that the eyes of the viewer perceive a continuous set of parallax images as the head is moved within the eyebox. Under this condition, the smooth motion parallax is guaranteed for those 3D images that exhibit at most one (perceived) display pixel disparity between the adjacent views [19]. Fig. 3 illustrates the maximum image distance z_s

from the display plane at which the motion parallax is perceived continuously. z_s can be simply found from similar triangles as

$$|z_s| = X_t \frac{d_v}{X_v - X_t}. \tag{4}$$

Please note that in practice various other factors affect the smoothness of the motion parallax. Cross-talk between the neighbor views constitutes the most significant of such factors. Indeed, as will be demonstrated in the experiments, if there exists significant cross-talk between the views, the motion parallax can be experienced smoothly even if none of above-mentioned conditions are satisfied.

Perceived Resolution

For a SMV display with a vertically positioned lenticular lens (i.e. the optical axis is vertical), the available pixel budget of the 2D display is shared between the number of views and the perceived resolution. Thus, the vertical perceived 3D image resolution is obtained to be the vertical display resolution, i.e. $N_{px} = N_x$; whereas the horizontal perceived resolution is found as the display resolution over the number of views, i.e.

$$N_{py} = \frac{N_y}{N_v}, \tag{5}$$

where N_y is the horizontal (2D) display resolution and N_v is the number of views within the eyebox. Noting that

$$N_v = \frac{W_v}{X_v} = \frac{X_t'}{X_y}, \tag{6}$$

the horizontal perceived resolution is given as

$$N_{py} = \frac{N_y X_y}{X_t'}. \tag{7}$$

Since the vertically placed lenticular lens results in uneven resolution loss in vertical and horizontal directions, it is usually preferred to place the lenticular lens with a slant angle, e.g. $\alpha = \arctan(1/6)$ [18]. With this arrangement, sub-pixels from different pixels are assigned to same view to form a perceived pixel, and thus the perceived horizontal resolution is increased at the expense of resolution loss in the vertical direction. Fig. 4 illustrates two example subpixel arrangements for a conventional LCD with RGB subpixels and lenticular lens with the slant angle of $\arctan(1/6)$. Note that in this configuration, X_t is given as $X_t = T_l/\cos(\alpha)$, where T_l is the lenticular pitch.

The slanted lens array arrangement actually corresponds to an equivalent non-slanted lens array configuration, where the effective pixel pitch X_y is equal to half of the subpixel pitch of the display δ_y, i.e. $X_y = \delta_y/2$. Thus, according to Eq. 5 and Eq. 6, slanted lens array placement can be used to double the number of views at the cost of halved horizontal resolution. For the configuration in Fig. 4a, the perceived horizontal and vertical resolution are then obtained as

$$N'_{py} = 3\frac{N_y \delta_y}{2X_t'}, \tag{8}$$

$$N'_{px} = \frac{N_x}{3}, \tag{9}$$

and for the configuration in Fig. 4b they are found as

$$N'_{py} = 6\frac{N_y \delta_y}{2X_t'}, \tag{10}$$

$$N'_{px} = \frac{N_x}{6}. \tag{11}$$

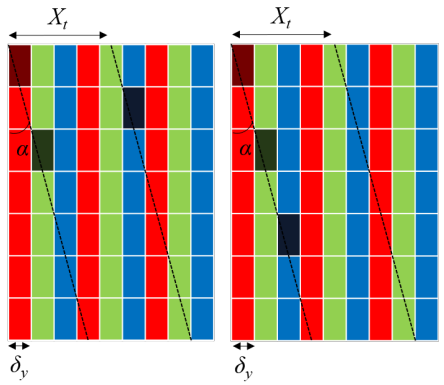

(a) (b)

Figure 4: Slanted lenticular configuration, when the resolution loss in the vertical dimension is by a factor of (a) 3 and (b) 6. The subpixels and the lens pitch are not drawn to scale.

Depth of Field of a SMV Display with Slanted Lens Array

The perceived resolutions discussed above are actually available within a limited depth range around the display surface, i.e. depth of field (DoF), and beyond that region the (spatial) resolution drops [20]. In this section, we briefly discuss this issue for the SMV-HUD using ray-space analysis, similar to [20], as it is relevant to specify the resolution limits for the intended virtual image depth.

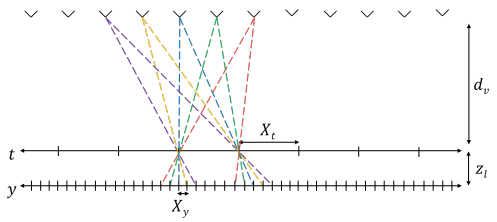

Figure 5: Ray sampling in SMV display (top view).

An example ray propagation diagram for the SMV-HUD system is illustrated in Fig. 5. The corresponding ray space diagram is given in Fig. 6a, where the $y-$coordinate is defined relative to the $t-$coordinate, i.e. $y-$coordinate of each pixel is defined with respect to the $t-$ coordinate of the corresponding lens. The slope of the sheared sampling grid is found as $s = z_l/d_v$.

The vertical shear in the (t,y) plane corresponds to a horizontal shear in the reverse direction in the Fourier domain [2]. Thus,

$$\mathscr{F}\{f(t,y+st)\} = F(\Omega_t - s\Omega_y, \Omega_y), \tag{12}$$

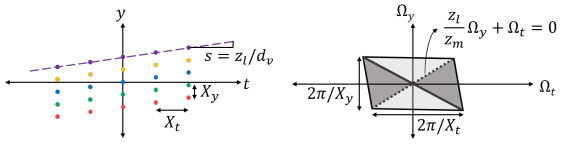

(a) (b)

Figure 6: Ray space analysis of SMV display. (a) Ray-space sampling grid, (b) display bandwidth.

where $F(\Omega_t, \Omega_y)$ represents the Fourier transform of $f(t,y)$. The bandwidth of the SMV display illustrated in Fig. 5 is, therefore, obtained to be a parallelogram as shown in Fig. 6b.

The display bandwidth shown in Fig. 6b allows representation of the scene in the depth range corresponding to dark gray at maximum spatial resolution [4]. The dashed diagonal line corresponds to the DoF boundary behind the display, whereas the solid one corresponds to the boundary in front of the display. We are interested in the boundary behind the display, which is obtained as

$$|z_m| = z_l \frac{X_t}{X_y - sX_t}. \tag{13}$$

Noting that $s = z_l/d_v$, the equation can be rewritten in the form of

$$|z_m| = \frac{d_v X_t}{X_y \frac{d_v}{z_l} - X_t}. \tag{14}$$

Please note that the constraint for the DoF is actually equivalent to the smooth motion parallax constraint given by Eq. 4. That is, $z_s = z_m$. As can be inferred from Fig. 6b, for depths beyond the DoF, i.e. $z > z_m$, the spatial resolution that can be shown by the display drops by the factor of z/z_m with respect to the maximum spatial resolution [20].

Experiments

Figure 7: Developed SMV-HUD demonstrator.

Our SMV-HUD demonstrator is shown in Fig 7. The SMV display is designed using a 16 lens-per-inch (LPI) lenticular lens slanted by the angle $\arctan(1/6)$, i.e. $X_t = 1.59mm$; and an RGB stripe LCD of size $16.9cm \times 25.4cm$ with subpixel pitches of $\delta_y = 39\mu m$ and $\delta_x = 117\mu m$, i.e. $X_y = 19.5\mu m$ and $X_x = 117\mu m$. The distance between lenticular and the LCD planes is $z_l = 4.25mm$. The viewer is assumed to be $d_v = 90cm$ away from the display. The eyebox is $W_v = 33.80cm$, where there are 82 views with distance of $X_v = 4.14mm$ between the neighbor views. The horizontal and vertical FOVs are 16° and 11°, respectively.

The subpixel mapping illustrated in Fig. 4b is employed, which results in the perceived resolution of 240×160 within the DoF of the display. The DoF is confined within the depth of $z_m = 55.95cm$ behind the display. Considering a virtual image distance e.g. $2.5m$ from the driver, the content is to be shown at $1.6m$ from the display plane, which is beyond the display DoF. Thus, at this particular depth, horizontal resolution reduces to around one third of the maximum spatial resolution.

The capability of the developed demonstrator is experimented in terms of the derived quality factors. In particular, the perceived resolution is evaluated at various distances, both inside and outside the display DoF. Verification of the perceived depth is done by testing the binocular cues and the smoothness of motion parallax. During the experiments, a camera of 1920×1200 pixels resolution is mounted on a linear positioning system that can be accurately moved in the horizontal and vertical directions. The camera is traced on the view points at $d_v = 90cm$ from the display plane to capture the necessary parallax images.

Perceived Resolution

We measure available spatial resolutions at depths inside and outside the DoF by presenting sinusoidal images at different frequencies. In particular, resolution tests are applied at $1.45m$, which is the edge of the display DoF, and at $3m$.

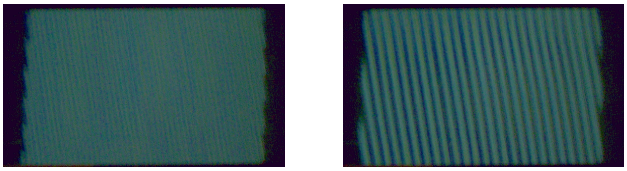

(a) (b)

Figure 8: Resolution test images at 1.45m away from the viewer. (a) Maximum resolution, (b) half of maximum resolution.

Fig. 8 illustrates two sinusoidal patterns captured at $1.45m$, by utilizing maximum spatial resolution (a) and half spatial resolution (b). That is, for instance in the case of Fig. 8a, the period of the sinusoid corresponds to two perceived pixel pitches. Please note that the orientation of the sinusoid is chosen to be aligned with the perceived pixel sampling pattern, i.e. it is rotated by the slant angle. It is observed in both Fig. 8a and Fig. 8b that the desired sinusoid images are correctly reconstructed by the display.

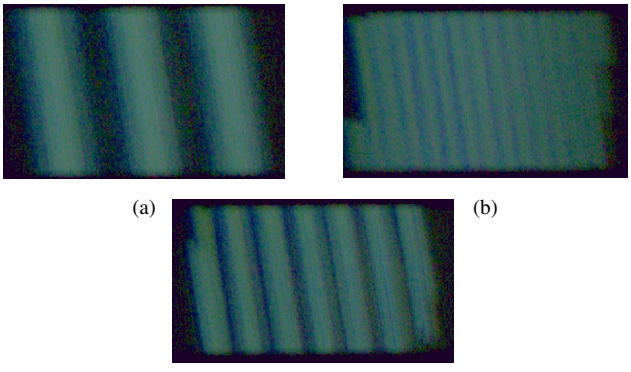

(a) (b)

(c)

Figure 9: Resolution test images at $3m$ away from the viewer. (a) Maximum spatial resolution, (b) reduced (available) resolution at $3m$, and (c) half of the available resolution at $3m$.

Fig. 9a illustrates captured images for three sinusoid images at different frequencies that correspond to (a) maximum spatial resolution, (b) reduced spatial resolution available at $3m$, i.e. reduced by the factor of $(3m-0.9m)/z_m$, and (c) half of the available resolution at $3m$. The aliased reconstructed image in Fig. 9a clearly indicates that at the depth of $3m$ the maximum spatial resolution cannot be achieved by the display. On the other hand, it is verified in Fig. 9b and Fig. 9c that the display is able to deliver resolutions up to the available (reduced) resolution at $3m$.

Perceived Depth

In order to test whether the binocular cues are delivered correctly, a test chart is placed at the distance of $3m$ from the camera, where the virtual image is displayed, and the relative motion parallax between the virtual image and the test chart is observed. Fig. 10 shows the captured images of the virtual image and the test chart from three different horizontal viewpoints. It can be observed that there is no relative motion parallax between the virtual image and the test chart, indicating that the image is correctly placed at the intendent depth and the multiview images deliver correct binocular cues. Negligible changes in the position and size of the virtual image is due to the manufacturing error in the lens array, such as skewness that distorts the parallel arrangement of the LCD and the lens plane.

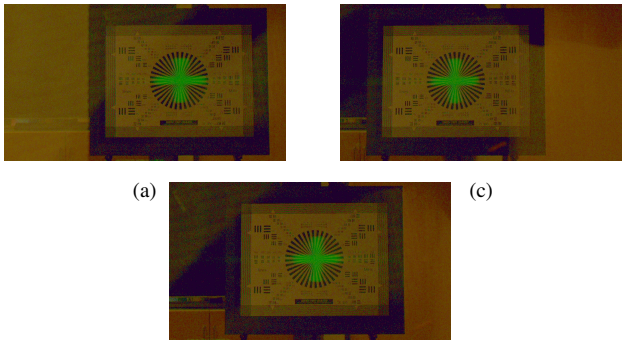

Figure 10: Images from different views for a test chart at $3m$. The camera is placed at (a) -10cm, (b) 0, and (c) 10cm with respect to the middle view. The contrasts of the images are enhanced for better visibility.

Motion parallax is another depth cue that should be delivered correctly and smoothly to provide comfortable driving conditions. Since the view pitch X_v is designed to be smaller than the average eye pupil size, smooth motion parallax is guaranteed for the images within the display DoF. However, the intended virtual HUD depths fall outside the DoF of our demonstrator, therefore rigorous validation of the motion parallax is required. Cross-talk between neighbor parallax images is a significant factor in this regard, which actually works in favor of smooth motion parallax. Therefore, below we analyze the cross-talk in our demonstrator.

In order to measure the cross-talk for a given view, the contributions of other views are to be measured at the corresponding view location. For this purpose, for each viewpoint, first a white image is displayed to the intended view and all other views are assigned black images. Camera is then moved along the views to measure the intensities. Fig. 11 shows the contributions of different views to neighbor views, where only the central 30-50th views are included for more clear illustration. The average cross-talk of the display (normalized intensity of a view image divided by total normalized intensities of all view images at the intended view location), is measured to be 32.5%, which introduces significant amount of blur in the angular dimension of the light field emitted by the SMV display.

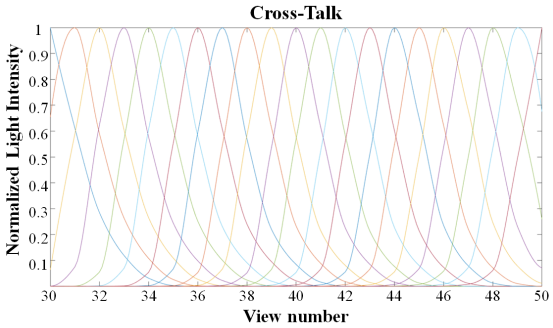

Figure 11: Cross-talk, interaction of views with each other.

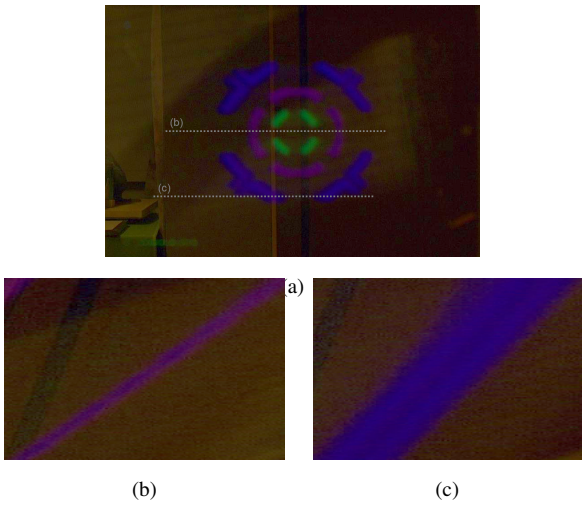

Figure 12: Smooth motion parallax test for a 3D scene consisting of different depth planes at $1.5m$, $2m$, and $3m$. (a) Captured image from the middle view (the image is cropped), (b)-(c) two example epipolar images for the rows shown in (a) that correspond to the depth planes at $2m$ and $3m$ respectively. The contrasts of the images are enhanced for better visibility.

Fig. 12a shows a virtual scene consisting of three circles at different depths, $1.5m$, $2m$, and $3m$. The smoothness of the motion parallax is illustrated in the epipolar images shown in Fig. 12b and Fig. 12c, i.e. there is a smooth transition along the rows that are constructed by vertically ordering the same rows of all view images. We also attach a video that is captured by moving the camera horizontally. The video consists of frames shot in every $2.5mm$. The smooth motion parallax for the inner circle is already satisfied by the condition that it is in the DoF of the display. Nevertheless, the smooth motion parallax is also maintained for the circles at $2m$ and $3m$, even if they are outside the DoF. The reasons are that there is significant amount of cross-talk in the system and also the patterns, especially outer ones, do not actually utilize maximum spatial resolution of the display.

Conclusion

We have proposed a virtual image HUD system based on the SMV display technique that is capable of displaying images at the typical virtual image HUD depths $2-3m$. Being capable of providing relevant physiological depth cues at the target virtual image distance with a thin form factor, SMV displays provide an attractive alternative solution to the existing HUD systems.

The presented theoretical analysis and experimental results demonstrate the trade-offs in the perceived spatial resolution, eyebox width, target image depth etc. In the developed demonstrator, for example, the eyebox could be kept smaller to increase the perceived resolution. Nevertheless, please note that the quality factors of the developed system can be improved significantly by utilizing recent display technology, which provides significantly higher resolution displays, and custom design lenticular lens. The recent developments in the active lens technology is expected to enable further improvements by utilizing time-multiplexed display techniques.

References

[1] J. R. Banbury. Head-up display systems. *Science Progress (1933-)*, pages 497–517, 1992.

[2] R. Bracewell. *The Two-Dimensional Fourier Transform*, pages 157–159. Springer US, Boston, MA, 2003.

[3] E. Buckley and D. Stindt. Full colour holographic laser projector hud. In *Proceedings: SID Annu. Symp. Veh. Displays*, volume 15, pages 131–135, 2008.

[4] J.X. Chai, X. Tong, S.C. Chan, and H.Y. Shum. Plenoptic sampling. pages 307–318. ACM, July 2000.

[5] J. Christmas, D. Masiyano, and N. Collings. Holographic automotive head up displays. *Electronic Displays Conference*, Feb 2015.

[6] K.W. Gish and L.K Staplin. *Human Factors Aspects of Using Head Up Displays in Automobiles: A Review of the Literature*. National Highway Traffic Safety Administration, 1995.

[7] M. K. Hedili, M. O. Freeman, and H. Urey. Microlens array-based high-gain screen design for direct projection head-up displays. *Appl. Opt.*, 52(6):1351–1357, Feb 2013.

[8] D. N. Jarrett. *Cockpit Engineering*. Ashgate Pub., 2005.

[9] Y. Kajiki. Ocular accommodation by super multi-view stereogram and 45-view stereoscopic display. *Proceedings of The Third International Display Workshops(IDW'96)*, 2:489–492, 1996.

[10] Yoshihiro Kajiki, Hiroshi Yoshikawa, and Toshio Honda. Hologramlike video images by 45-view stereoscopic display. volume 3012, pages 154–166, 1997.

[11] R.J. Kiefer. Quantifying head-up display (hud) pedestrian detection benefits for older drivers. In *Proceedings: International Technical Conference on the Enhanced Safety of Vehicles*, pages 428–437, 1998.

[12] R.J. Kiefer and A.W. Gellatly. Quantifying the consequences of the 'eyes-on-road' benefit attributed to head-up displays. In *SAE Technical Paper*. SAE International, 02 1996.

[13] N. S Martinelli and S. A Boulanger. Cadillac deville thermal imaging night vision system. Technical report, SAE Technical Paper, 2000.

[14] K. Nakamura, J. Inada, M. Kakizaki, T. Fujikawa, S. Kasiwada, H. Ando, and N. Kawahara. Windshield display for intelligent transport system. In *11th World Congress on Intelligent Transportation Systems*, volume 85, pages 3058–3065, 2004.

[15] Takanori Okoshi. *Three-dimensional imaging techniques*. Elsevier, 2012.

[16] Y. Takaki, Y. Urano, S. Kashiwada, H. Ando, and K. Nakamura. Super multi-view windshield display for long-distance image information presentation. *Opt. Express*, 19(2):704–716, Jan 2011.

[17] T. Todoriki, J. Fukano, S. Okabayashi, M. Sakata, and H. Tsuda. Application of head-up displays for in-vehicle navigation/route guidance. In *Proceedings: Vehicle Navigation and Information Systems Conference*, pages 479–484, Aug 1994.

[18] C. van Berkel. Image preparation for 3d lcd. In *Proc. SPIE*, volume 3639, pages 84–91, 1999.

[19] M. Yamaguchi. Light-field and holographic three-dimensional displays. *JOSA A*, 33(12):2348–2364, 2016.

[20] M. Zwicker, W. Matusik, F. Durand, and H. Pfister. Antialiasing for automultiscopic 3d displays. In *ACM SIGGRAPH 2006 Sketches*, page 107. ACM, 2006.

JOIN US AT THE NEXT EI!

IS&T International Symposium on

Electronic Imaging

SCIENCE AND TECHNOLOGY

Imaging across applications . . . Where industry and academia meet!

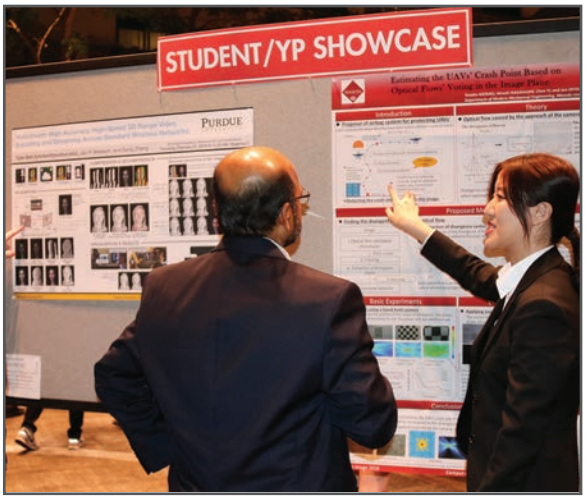

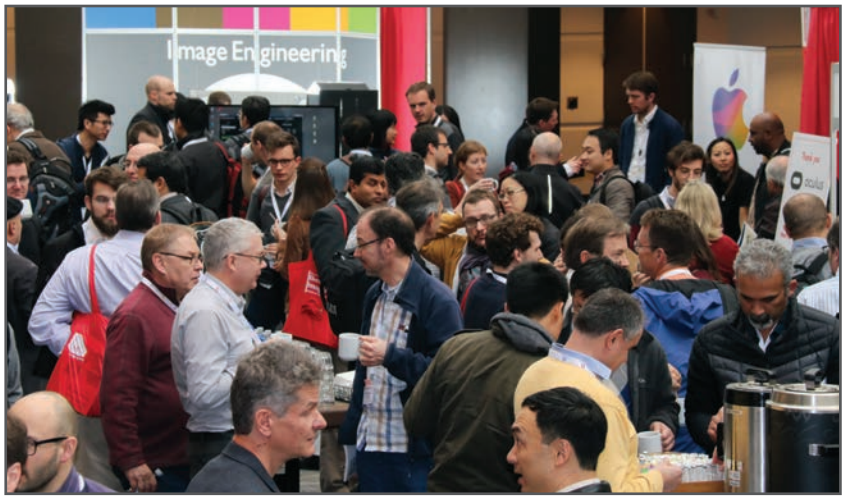

• SHORT COURSES • EXHIBITS • DEMONSTRATION SESSION • PLENARY TALKS •
• INTERACTIVE PAPER SESSION • SPECIAL EVENTS • TECHNICAL SESSIONS •

www.electronicimaging.org

IS&T
imaging.org